Headache
© 2017 American Headache Society
ISSN 0017-8748
doi: 10.1111/head.13231
Published by Wiley Periodicals, Inc.

Brief Communications

Antagonistic Relationship Between VEP Potentiation and Gamma Power in Visual Snow Syndrome

Sebastian Luna, BA; Daniel Lai; Alison Harris, PhD

Objective.—Using a "double-pulse" adaptation paradigm, in which two stimuli are presented in quick succession, this study examines the neural mechanisms underlying potentiation of the visual evoked potential (VEP) in visual snow syndrome.

Background.—Visual snow is a persistent visual disturbance characterized by rapid flickering dots throughout the visual field. Like the related condition of migraine with aura, visual snow has been hypothesized to arise from abnormal neuronal responsiveness, as demonstrated by a lack of typical VEP habituation to repeated visual stimulation. Yet the exact neural mechanisms underlying this effect remain unclear. Previous "double-pulse" experiments suggest that typical VEP habituation reflects disruptive gamma-band (50-70 Hz) neural oscillations, possibly driven by inhibitory interneurons. Given that migraine has been associated with reduced cortical inhibition, we propose here that visual snow may likewise reflect diminished inhibitory activity, resulting in decreased gamma power following initial visual stimulation and concomitant potentiation of the subsequent VEP response.

Methods.—We compared VEP responses to double-pulse adaptation in a 22-year-old man with a 2-year history of visual snow versus a group of age- and gender-matched controls ($N = 5$). The patient does not have a comorbid diagnosis of episodic migraine or migraine with aura, and controls had no personal or family history of migraine.

Results.—In contrast to the pattern of habituation observed in controls, visual snow was associated with persistent potentiation of the VEP response. Consistent with our predictions, time-frequency analysis revealed reduced gamma-band power following the initial stimulus in visual snow relative to controls.

Conclusions.—These results support an antagonistic interplay between gamma power and rapid neural adaptation, shedding new light on the neural mechanisms of VEP potentiation in visual snow.

Key words: event-related potentials, double-pulse adaptation, P100 response, time-frequency analysis

(*Headache* 2018;58:138-144)

Positive visual phenomena, in which patients experience illusions or distortions of visual perception, provide a window on the consequences of abnormal neural responsiveness in pathological states. Although the neural mechanisms of positive visual phenomena have been studied extensively in the context of migraine aura,[1] less is known about the underlying pathology in "visual snow," a related but distinct visual disorder.[2] Individuals with visual snow report a persistent and ongoing visual disturbance in the entire visual field, characterized by rapid flickering of fine dots resembling video noise or "static."[2,3]

Like migraine, visual snow has been hypothesized to arise from changes in the responsiveness of

From the Department of Neuroscience, W.M. Keck Science Department, Claremont, CA, USA (S. Luna, D. Lai, and A. Harris); Department of Psychology, Claremont McKenna College, Claremont, CA, USA (A. Harris).

Address all correspondence to A. Harris, PhD, Department of Psychology, Claremont McKenna College, 850 Columbia Avenue, Claremont, CA 91711, USA, email: aharris@cmc.edu

Accepted for publication October 13, 2017.

Conflicts of Interest: None.

neurons to sensory stimulation.[3] Measurements of visual evoked potentials (VEPs) in normal individuals typically show physiological habituation, a decrease in neural response to repeated stimulus presentations.[4] In contrast, VEPs to repeated stimulation are often potentiated, or increased, in patients with migraine.[5] Consistent with this idea, a recent study reported VEP potentiation associated with visual snow.[6] However, these results have been questioned due to the patient's prior history of migraine with aura,[7] as well as more general concerns about the reliability of VEP habituation in migraine.[8]

Here, we tested VEP habituation in a 22-year-old male visual snow patient without comorbid migraine, ruling out underlying migraine with aura as a confounding factor. Additionally, we extend previous research by measuring VEP habituation using a rapid "double-pulse" adaptation paradigm in which two stimuli (S1 and S2) are presented with a variable stimulus onset asynchrony (SOA). Adaptation to double-pulse presentations has been observed for signals arising from both early visual cortex[9] and higher-order perceptual areas,[10] and can be elicited by paired presentations of different images, suggesting it does not solely depend on low-level physical stimulus properties.[11,12] Rather than indexing a direct reduction of neural activity, this adaptation effect appears to reflect disruption of the S2 response by synchronized gamma-band (50-70 Hz) oscillations preceding the onset of the S2 stimulus, with greater suppression of the evoked S2 response associated with higher pre-S2 gamma power.[13]

One possible neural mechanism for the disruptive effect of pre-S2 gamma comes from previous work showing that synchronous cortical gamma oscillations depend on the activity of inhibitory interneurons.[14] Interestingly, inhibition of visual cortex appears to be diminished in migraine, as evidenced by studies using metacontrast masking[15] and noninvasive brain stimulation.[16] Thus, we hypothesize that in visual snow, reduced inhibition of visual cortices would lead to decreased synchronous gamma oscillations (ie, lower power) preceding the S2 stimulus, relative to normal levels, with a concomitant lack of VEP habituation.

METHODS

The patient is a right-handed 22-year-old male with a 2-year history of visual snow syndrome. He meets the recently proposed diagnostic criteria for visual snow,[2] chief of which is the experience of constantly flickering fine dots throughout the entire visual field. This symptom persists in all light conditions and when the eyes are closed. The patient also experiences several related positive sensory phenomena, including palinopsia, nyctalopia, photopsia, phosphenes, the blue field entopic phenomenon, and tinnitus. All symptoms developed over the course of two weeks and have since persisted without remission. The patient has normal visual acuity and eye structure, and no abnormalities have been detected in neurological and neuroimaging examinations.

Given that five past headache attacks of migrainous phenotype are sufficient for a diagnosis of episodic migraine, it is important to quantify the number and extent of previous migraine episodes. The patient has experienced one attack of migrainous phenotype with stereotypical symptoms of migraine aura, which occurred 6 years prior to this study. The patient has not experienced any other migraine attacks. Therefore, the patient does not qualify for a diagnosis of episodic migraine. However, there is a family history of migraine with aura on the maternal side.

Seven gender- and age-matched controls (ages 20-24, mean age = 21.1) were recruited from the college community, of whom two were excluded due to problems with EEG recording. All control participants had normal or corrected vision and no personal or family history of migraine. Informed consent was obtained from all participants, and the study was approved by the college's Institutional Review Board.

In the double-pulse adaptation experiment, two stimuli were presented for 17 ms each with four SOAs: 50, 67, 117, and 217 ms (Fig. 1A). Stimuli consisted of 50 high-contrast black-and-white line patterns (4.6° × 4.6° of visual angle), presented on a gray background with a central fixation point[11] (Fig. 1B). Subjects monitored for an infrequent checkerboard target (10% of total trials), the

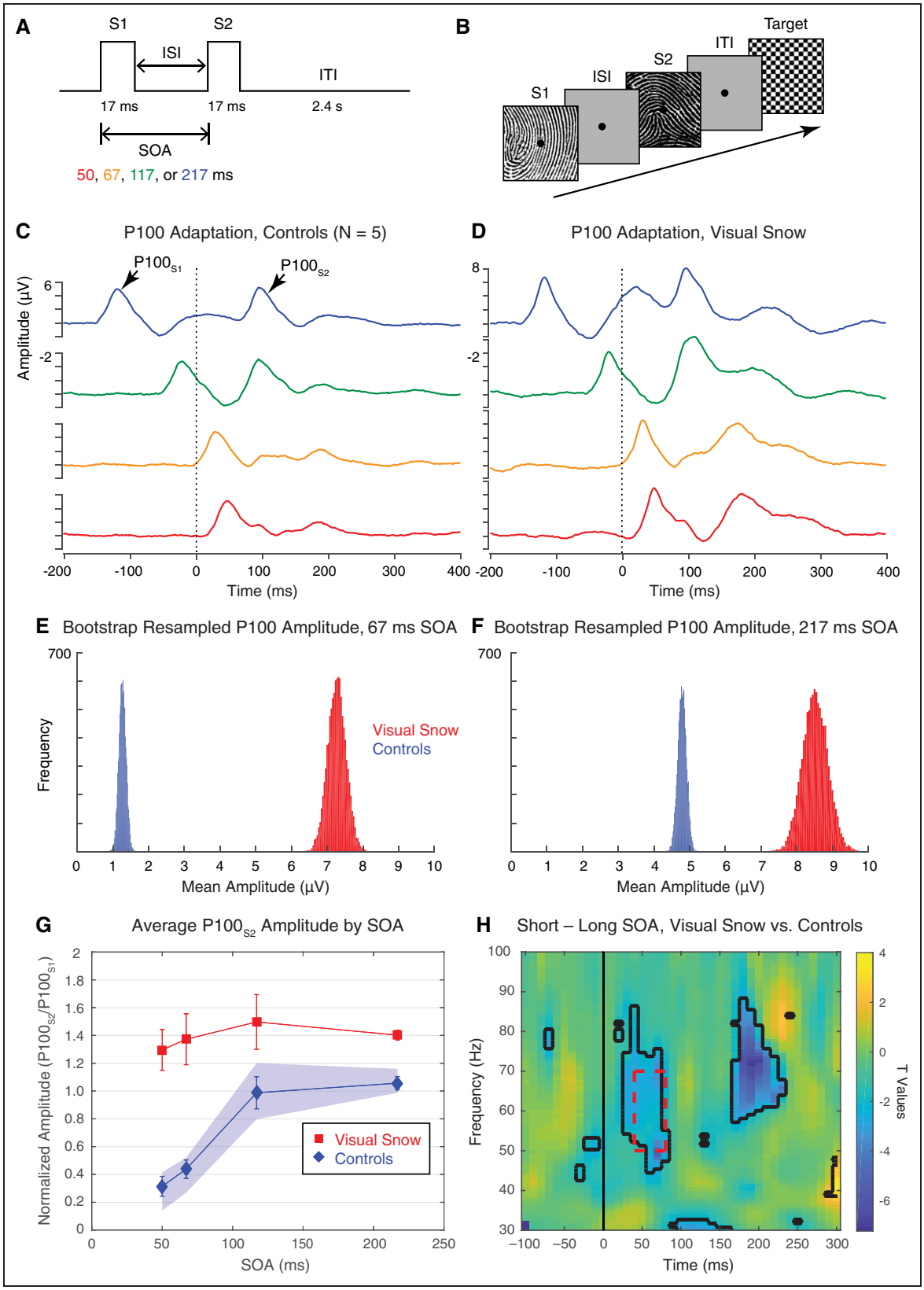
A
S1
S2
ISI
ITI
17 ms
17 ms
2.4 s
SOA
50, 67, 117, or 217 ms
B
Target
ITI
S2
ISI
S1
C
P100 Adaptation, Controls (N = 5)
P100S1
P100S2
Amplitude (μV)
Time (ms)
D
P100 Adaptation, Visual Snow
Time (ms)
E
Bootstrap Resampled P100 Amplitude, 67 ms SOA
Frequency
Visual Snow
Controls
Mean Amplitude (μV)
F
Bootstrap Resampled P100 Amplitude, 217 ms SOA
Mean Amplitude (μV)
G
Average P100S2 Amplitude by SOA
Normalized Amplitude (P100S2/P100S1)
Visual Snow
Controls
SOA (ms)
H
Short – Long SOA, Visual Snow vs. Controls
Frequency (Hz)
Time (ms)
T Values

Fig. 1.

appearance of which was randomly intermixed with the experimental trials. All trials were programmed and displayed in Matlab (Mathworks, Natick, MA, USA) using PsychToolbox[17] stimulus presentation software.

EEG data were collected using a 128-channel BioSemi ActiveTwo system (Biosemi B.V., Amsterdam, Netherlands), digitized continuously at 512 Hz with bilateral mastoid references. Offline data processing was performed using the EEGLAB toolbox,[18] including re-sampling to 500 Hz, re-referencing to an average reference, linear detrending, high-pass filtering at 1 Hz, notch filtering at 60 Hz, and selection of epochs time-locked to the S1 stimulus (–500 ms to 800 ms). Artifactual noise was identified and removed using independent components analysis[19] via second-order blind identification,[20] and 600-ms epochs time-locked to the S2 stimulus (–200 ms to 400 ms) were extracted. Preprocessing for time-frequency followed a similar procedure, but excluding re-referencing and filtering of the data.

To measure VEP adaptation, we examined the P100 response, occurring approximately 100 ms post-stimulus onset at posterior sensors. For each participant, individual sensors of interest (SOIs) were defined 90-110 ms post-stimulus onset at posterior sensors based on the amplitude of VEPs to the S1 stimulus, using a threshold of z-scored amplitude ≥ 1.5. Local peak amplitude and latency for the S2 response were then determined for each participant and condition using a 10-point (20-ms) window in the ERPLAB[21] toolbox for Matlab. To ensure that these subject-level averages were not disproportionately influenced by a small number of outlying values, we empirically estimated the mean amplitude of the $P100_{S2}$ response for a 20-ms window (10 ms pre-, 10 ms post-) around the average peak latency in the 67 and 217 ms SOA conditions based on the individual trial data using a bootstrapping procedure (1,000 permutations). Bootstrap estimates were computed separately across controls in order to preserve inter-subject variability. The extent of adaptation was quantified by normalizing the P100 response to the S2 stimulus by the amplitude of the preceding S1 response ($P100_{S2}/P100_{S1}$). Bootstrap confidence intervals for the normalized $P100_{S2}$ response were constructed using 10,000 permutations resampling the original subject-level data with replacement.

Time-frequency analysis was performed using the FieldTrip toolbox[22] for Matlab using a Morlet wavelet (width = 7). Time-frequency analysis was performed individually in each participant for all trials, averaging across the participant's individually defined SOIs. We first computed the difference in power between Short and Long SOA, defined by 67 ms versus 217 ms SOA respectively, within participant. We then compared the difference of Short–Long SOA in visual snow versus

Fig. 1.—(A) Schematic of the "double-pulse" adaptation paradigm. Two stimuli, S1 and S2, are presented for 17 ms each with a variable interstimulus interval (ISI) from 33 to 200 ms, producing stimulus onset asynchronies (SOAs) of 50, 67, 117, and 217 ms. Following S2, a fixation point was displayed for an intertrial interval (ITI) of 2.4 s, chosen to minimize persistent afterimages between trials in the visual snow patient. (B) Double-pulse adaptation of the early visual P100 component. On each trial, two of 50 high-contrast black-and-white (fingerprint) stimuli were selected and presented in pairs, with each pattern serving as the S2 image twice per condition (100 trials per condition). A nonidentical image was randomly selected as S1. Participants were instructed to respond to the appearance of an infrequent target image (checkerboard pattern), which occurred on 10% of trials. (C-D) P100 adaptation in (C) control participants and (D) visual snow patient across four SOAs (colors as indicated in A). Grand average waveforms are time-locked to the onset of the S2 stimulus (dotted line, 0 ms), with the $P100_{S2}$ response occurring approximately 100 ms after stimulus onset. Note that at shorter SOAs the $P100_{S1}$ is visible in the time leading up to the $P100_{S2}$. Grand averages in (D) reflect the average of two separate sessions in the visual snow patient. (E-F) Bootstrap resampled mean amplitudes of the $P100_{S2}$ response for the (E) 67 ms SOA and (F) 217 ms SOA conditions. Mean amplitudes were computed for each trial in each subject for a 20-ms window around the average peak latency, and distributions of bootstrapped means were derived from 1,000 samples with replacement from the trial data within subject. (G) Average normalized $P100_{S2}$ amplitude by SOA for visual snow patient (red squares) versus controls (blue diamonds). Error bars represent the standard error of the mean. The shaded blue area indicates 95% confidence intervals, as determined by bootstrapping (10,000 permutations). (H) Time-frequency analysis of Short–Long SOA in visual snow versus controls. Red dashed box: Time-frequency window of interest in which gamma power differences were predicted. Black outlines indicate windows in which *t* values were significant, corrected for multiple comparisons using the false discovery rate (FDR).

control participants using an independent-samples two-tailed t test with a nonparametric Monte Carlo permutation statistic (10,000 repetitions). Results were corrected for multiple comparisons via the false discovery rate (FDR). Based on our a priori hypotheses, we predicted that significant reductions in gamma power would be visible in the time window preceding the $P100_{S2}$ response (40 to 80 ms post-stimulus) in the frequency range of 50 to 70 Hz.

RESULTS

Grand average waveforms in controls (Fig. 1C) and the visual snow patient (Fig. 1D) revealed recognizable P100 components in response to the S1 and S2 stimuli. The pattern in controls replicated earlier findings[9,11] of decreasing adaptation at longer SOAs, with full recovery of P100 amplitude by 117 ms SOA on average (Fig. 1C). In contrast, across two separate recording sessions, the visual snow patient showed a distinctive pattern of adaptation characterized by marked potentiation of the $P100_{S2}$ response (Fig. 1D). Although measurement of the $P100_{S2}$ response at shorter SOAs was complicated by the atypical appearance of the VEP waveform, we focused on the first positive peak following the $P100_{S1}$ (mean latency: 50 ms SOA = 181.7 ms, 67 ms SOA = 172 ms) due to the patient's report of prolonged afterimages following visual stimulation, as well as the observation that even for an SOA of 117 ms, the patient's average $P100_{S2}$ response showed a delayed peak latency relative to those of controls ($t(4) = -8.47$, $P = 0.001$, one-sample t test). To ensure that the differences between average waveforms in the controls and patient were not driven by a small number of outlying trials, we further reconstructed the distribution of mean $P100_{S2}$ amplitudes for two of the SOA conditions, 67 ms (Fig. 1E) and 217 ms (Fig. 1F), using a bootstrap resampling procedure on individual trial data (1,000 permutations). Comparison of the bootstrap resampled mean P100 amplitude across controls (blue) versus within the patient (red) indicated that the two distributions were completely separated, with higher mean amplitudes for the patient regardless of SOA condition.

Looking across the full range of tested SOAs, adaptation effects in the visual snow patient were strikingly reduced in comparison to controls (Fig. 1G). Bootstrap resampled 95% confidence intervals (Fig. 1G, shaded blue area) revealed no overlap between control and patient averages. To confirm this result statistically, we conducted a mixed-design ANOVA with visual snow as a between-subjects factor and SOA as a repeated measure. Degrees of freedom were adjusted to correct for violations of sphericity by the average estimated epsilon from Greenhouse-Geisser and Hunyh-Feldt corrections.[23] The analysis revealed a significant main effect of SOA ($F(2.05,8.2) = 8.79$, $P = 0.009$) within subjects, as well as a significant interaction of SOA x Visual Snow ($F(2.05,8.2) = 4.33$, $P = 0.05$) and between-subjects effect of Visual Snow: ($F(1,4) = 23.2$, $P = 0.009$).

We further hypothesized that this lack of habituation would be correlated with reduced gamma power in the time preceding the second stimulus. For each participant, we computed gamma power associated with long versus short SOA (217 versus 67 ms) from −100 to 400 ms after onset of the second stimulus. We hypothesized that, in the time directly preceding the onset of the S2 response, controls would show a positive effect (ie, greater disruptive gamma power in the short SOA condition), whereas the visual snow patient would have a negative or null effect. Comparing visual snow minus controls, we therefore expected a negative effect between 50 and 70 Hz,[13] occurring roughly 40 to 80 ms after S2 stimulus onset (Fig. 1F, red dashed box). In line with this prediction, an independent-samples t test using a nonparametric Monte Carlo permutation statistic (10,000 permutations) found significant negative t values overlapping with the a priori time-frequency window of interest (Fig. 1F).

DISCUSSION

Despite growing awareness of visual snow as a distinct disorder from migraine with aura, the neural underpinnings of this condition remain unclear. Here we addressed this question by measuring

VEP response habituation using a "double-pulse" paradigm.[9-12] Our results replicate previous findings of VEP potentiation in visual snow syndrome,[6] further demonstrating this effect in the absence of comorbid migraine with aura. This potentiation effect was visible across a range of tested SOAs, and persisted beyond the recovery from adaptation observed in control participants. Because all SOA conditions were randomly interleaved, rather than presented in successive blocks, the observed difference is unlikely to be explained by confounding factors such as fluctuations in attention or increasing fatigue.[7,8]

More significantly, our data provide a novel mechanistic link between VEP potentiation and neural oscillations in the gamma band. In line with previous research,[13] we observed an antagonistic relationship between pre-S2 gamma power and the subsequent evoked response, with reduced gamma synchronization in visual snow. Although the origins of this effect are not completely understood, inhibitory interneurons appear to play a key role in driving gamma oscillations, thereby gating cortical sensory responses.[14] In this light, reported hypermetabolism in the visual cortices of patients with visual snow[24] is consistent with diminished inhibitory processes.

Our results parallel an extensive literature on VEP habituation in migraine, which has been variously ascribed not only to decreased inhibition,[16] but also to increased cortical excitability or reduced pre-activation levels.[5] While we cannot rule out these alternative explanations for the VEP potentiation observed here, our results highlight an important role for time-frequency analysis in interpreting the evoked potential data. In particular, the emergence of antagonistic gamma synchronization in the time window following the $P100_{S1}$ response points to a specific role of local recurrent circuits in mediating double-pulse adaptation. Lower synchrony of neural oscillations in this time period may interact with reduced baseline activity levels and/or neuronal hyperexcitability to allow greater synchronization of the response to the subsequent S2 stimulus, leading to the VEP potentiation observed here.

Finally, although our data are highly consistent with the substantial scientific literature on "double-pulse" adaptation, further research will be necessary to confirm these findings. For example, despite currently lacking symptoms of migraine with aura, our visual snow patient has had a previous migrainous attack with aura and thus may qualify for this diagnosis in the future. More generally, comparison of larger patient samples to controls matched for migraine and aura, along with assessment of other visual evoked potentials, will be necessary to disentangle the neurological factors contributing to visual snow, as well as relating them to the severity and persistence of associated positive visual phenomena.

CONCLUSIONS

Collectively, these findings provide new insights into the physiological basis of positive visual phenomena in visual snow. Future research examining double-pulse adaptation for larger patient samples and additional visual evoked components has the potential to shed further light on the physiological correlates of this debilitating condition.

Acknowledgments: The authors thank Aleena Young for her insightful comments on a previous version of the manuscript.

STATEMENT OF AUTHORSHIP

Category 1

(a) Conception and Design
Sebastian Luna, Alison Harris

(b) Acquisition of Data
Sebastian Luna, Daniel Lai, Alison Harris

(c) Analysis and Interpretation of Data
Daniel Lai, Alison Harris

Category 2

(a) Drafting the Manuscript
Sebastian Luna, Daniel Lai, Alison Harris

(b) Revising It for Intellectual Content
Sebastian Luna, Alison Harris

Category 3

(a) Final Approval of the Completed Manuscript
Sebastian Luna, Daniel Lai, Alison Harris

REFERENCES

1. Lauritzen M. Pathophysiology of the migraine aura: The spreading depression theory. *Brain.* 1994;117:199-210.
2. Schankin CJ, Maniyar FH, Digre KB, Goadsby PJ. 'Visual snow' - a disorder distinct from persistent migraine aura. *Brain.* 2014;137:1419-1428.
3. Lauschke JL, Plant GT, Fraser CL. Visual snow: A thalamocortical dysrhythmia of the visual pathway? *J Clin Neurosci.* 2016;28:123-127.
4. Megela AL, Teyler TJ. Habituation and the human evoked potential. *J Comp Physiol Psychol.* 1979;93:1154-
5. Coppola G, Pierelli F, Schoenen J. Habituation and migraine. *Neurobiol Learn Memory.* 2009;92: 249-259.
6. Unal-Cevik I, Yildiz FG. Visual snow in migraine with aura: Further characterization by brain imaging, electrophysiology, and treatment–case report. *Headache.* 2015;55:1436-1441.
7. Fantini J, Sartori A, Manganotti P. Can we speak of lack of habituation in visual snow? *Headache.* 2016;56:1517-1518.
8. Omland PM, Uglem M, Hagen K, Linde M, Tronvik E, Sand T. Visual evoked potentials in migraine: Is the "neurophysiological hallmark" concept still valid? *Clin Neurophysiol.* 2016;127:810-816.
9. Musselwhite M, Jeffreys D. Visual evoked potentials to double-pulse pattern presentation. *Vis Res.* 1983;23:135-143.
10. Jeffreys DA. Evoked potential studies of face and object processing. *Vis Cogn.* 1996;3:1-38.
11. Harris A. Face-selectivity of the M170 response in developmental prosopagnosia and double-pulse adaptation. PhD Dissertation. 2005.
12. Harris A, Nakayama K. Rapid face-selective adaptation of an early extrastriate component in MEG. *Cereb Cortex.* 2007;17:63-70.
13. Privman E, Fisch L, Neufeld MY, et al. Antagonistic relationship between gamma power and visual evoked potentials revealed in human visual cortex. *Cereb Cortex.* 2011;21:616-624.
14. Cardin JA, Carlen M, Meletis K, et al. Driving fast-spiking cells induces gamma rhythm and controls sensory responses. *Nature.* 2009;459:663-667.
15. Palmer JE, Chronicle EP, Rolan P, Mulleners WM. Cortical hyperexcitability is cortical underinhibition: Evidence from a novel functional test of migraine patients. *Cephalalgia.* 2000;20:525-532.
16. Brighina F, Palermo A, Fierro B. Cortical inhibition and habituation to evoked potentials: Relevance for pathophysiology of migraine. *J Headache Pain.* 2009;10:77-84.
17. Brainard DH. The psychophysics toolbox. *Spat Vis.* 1997;10:433-436.
18. Delorme A, Makeig S. EEGLAB: An open source toolbox for analysis of single-trial EEG dynamics including independent component analysis. *J Neurosci Methods.* 2004;134:9-21.
19. Jung TP, Makeig S, Humphries C, et al. Removing electroencephalographic artifacts by blind source separation. *Psychophysiology.* 2000;37:163-178.
20. Belouchrani A, Abed-Meraim K, Cardoso J-F, Moulines E. A blind source separation technique using second-order statistics. *IEEE Trans Sig Process.* 1997;45:434-444.
21. Lopez-Calderon J, Luck SJ. ERPLAB: An open-source toolbox for the analysis of event-related potentials. *Front Hum Neurosci.* 2014;8:213.
22. Oostenveld R, Fries P, Maris E, Schoffelen JM. FieldTrip: Open source software for advanced analysis of MEG, EEG, and invasive electrophysiological data. *Comput Intell Neurosci.* 2011;2011: 156869-
23. Stevens J, *Applied Multivariate Statistics for the Social Sciences*. Hillsdale, NJ: Lawrence Erlbaum Associates; 1992.
24. Schankin CJ, Maniyar FH, Sprenger T, Chou DE, Eller M, Goadsby PJ. The relation between migraine, typical migraine aura and "visual snow." *Headache.* 2014;54:957-966.